Drift compression of an intense neutralized ion beam

P. K. Roy, S. S. Yu, E. Henestroza, A. Anders, F. M. Bieniosek, J. Coleman, S. Eylon, W. G. Greenway, M. Leitner, B. G. Logan and W. L. Waldron
Lawrence Berkeley National Laboratory, 1 Cyclotron Road, Berkeley, CA-94720, U.S.A

D. R. Welch and C. Thoma
ATK Mission Research, Albuquerque, New Mexico 87110-3946, U.S.A

A. B. Sefkow, E. Gilson, P. C. Efthimion and R. C. Davidson
Princeton Plasma Physics Laboratory, New Jersey 08543-0451, U.S.A.
(Dated: September 1, 2005)

Longitudinal compression of a tailored-velocity, intense neutralized ion beam has been demonstrated. The compression takes place in a 1-2 m drift section filled with plasma to provide space-charge neutralization. An induction cell produces a head-to-tail velocity ramp that longitudinally compresses the neutralized beam, enhancing the beam peak current by a factor of 50 and producing a pulse duration of about 3 ns. This measurement has been confirmed independently with two different diagnostic systems.

PACS numbers: 28.52, 29.17, 29.20, 29.27, 28.52, 41, 52, 94.20, 94.30

The simultaneous transverse and longitudinal compression of an ion beam is required to achieve the high intensities necessary to create high energy density matter and fusion conditions. A recent driver study for inertial fusion, for example, requires that 120 Bi^+ beams, each of ~50 kJ, be focused onto the target with small focal spot sizes of radius < 2 mm, and pulse lengths of ~ 10 ns [1, 2]. Simulations showed that these small spot sizes could be achieved with plasma neutralization [3, 4]. A scaled experiment, the Neutralized Transport Experiment (NTX) [5–8], subsequently demonstrated that an un-neutralized beam of several centimeter radius can be compressed transversely to ~1 mm radius when charge neutralization by background plasma electrons is provided, in quantitative agreement with the simulation [9, 10].

Longitudinal compression of space-charge-dominated beams has been studied extensively in theory and simulations [11–16]. The compression is initiated by imposing a linear head-to-tail velocity tilt to a drifting beam. Longitudinal space-charge forces limit the beam compression ratio, the ratio of the initial to final current, to about ten in most applications. An experiment with five fold compression has been reported [17].

Recent theoretical models and simulations predict that much higher compression ratios (≤100) could be achieved if beam compression takes place in a neutralized drift region [18, 19]. To experimentally study the effects of plasma neutralization on beam compression, the Neutralized Drift Compression Experiment (NDCX) was constructed at the Lawrence Berkeley National Laboratory. Figure 1 shows a schematic of the NDCX beam line. The NDCX experiment uses the same front end as the earlier NTX experiment. It consists of a 300 keV, 25-milliamp K^+ beam from an alumino silicate source powered by a Marx generator. Four pulsed quadrupoles magnets used in NTX to control the beam envelope (beam radius and convergence angle) are retained for the present experiments on NDCX. To provide the head-to-tail velocity tilt, an induction module with variable voltage waveform is placed immediately downstream of the last quadrupole magnet. This is followed by a neutralized drift section which consists of a one -meter-long plasma column produced by an Al cathodic arc [20]. A diagnostic box is located at the downstream end of the plasma column.

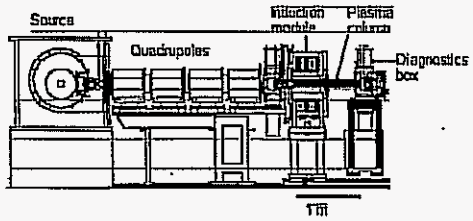

FIG. 1: Schematic of the NDCX experimental setup.

The beam produced from the source has a 6 μs flat-top. The induction tilt voltage 'carves' out a ~300 ns segment of the flat-top which compresses longitudinally as it drifts through the plasma column. The final compressed beam is measured in the downstream diagnostic box.

The induction cell consists of 14 independently-driven magnetic cores in a pressurized gas (SF_6) region that is separated from the vacuum by a conventional high voltage insulator. The waveforms applied to the 14 cores inductively add at the acceleration gap. Each core is driven by a thyratron-switched modulator. Because the modulator for each core can be designed to produce different waveforms and can be triggered independently, a variety of waveforms can be produced at the acceleration gap using the 14 discrete building blocks.

The plasma column is formed by two pulsed aluminum cathodic arc sources located at the downstream end. Each source is equipped with a 45^0 open-architecture

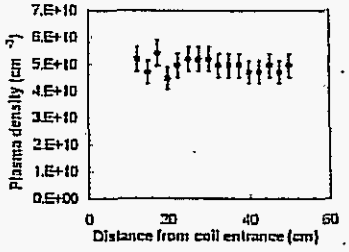

FIG. 2: Axial aluminum plasma density in the plasma column measured with a movable probe.

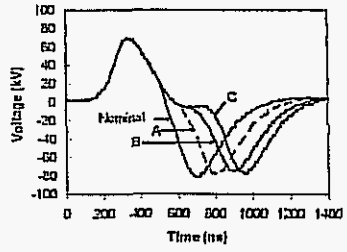

FIG. 3: Induction module voltage waveforms produced by varying the timing of the modulators.

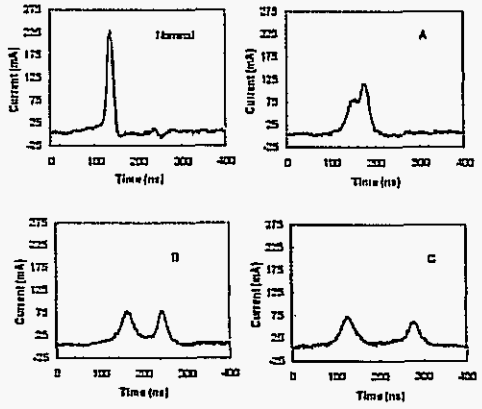

FIG. 4: Neutralized drift-compressed beam current with the voltage waveforms in Fig.3.

macroparticle filter providing a flow of fully ionized aluminum plasma [21]. The two plasma flows were pointed at an angle of 45^0 towards the solenoidal column ($\sim$ 1kG, 7.6 cm diameter, and 1 m long). A significant fraction (>10%) of the plasma enters the solenoid, and drifts practically unattenuated through the entire column (the rest of the aluminum plasma condenses at the wall and thereby removed from the system). Figure 2 shows the plasma density measured with a biased probe within the plasma column. In most of the operating regimes, the plasma density is at least a factor of 10 higher than the beam density. At the upstream end of the column, we have introduced a 'plasma stopper' consisting of two opposing dipoles of $\sim$1kG each, which inhibit the motion of plasma upstream into the induction gap and quadrupole focusing sections. A second plasma column consisting of a meter-long ferro-electric plasma source that does not require solenoidal confinement has been constructed and is undergoing experimental tests.

A phototube diagnostic [22] is used to measure beam pulse compression with and without neutralization by background plasma. The optical system is based on a Hamamatsu phototube with fast (sub-ns) response which is coupled to a 500-MHz oscilloscope. The beam pulse is measured by using the phototube to collect the optical photon flux from an aluminum oxide scintillator placed in the path of the beam. The time response of the scintillator is fast enough to make measurements on a nanosecond time scale. Small amounts of stray light emitted by the plasma over long periods of time (100s of μs) can drain the bias charge in the phototube's internal power supply, and thus spoil the gain of the phototube during the beam pulse. This background plasma light is blocked from entering the phototube by an electro-optic gated shutter (Displaytech) that opens just before the beam pulse arrives at the scintillator. The scintillator itself is not sensitive to low-energy plasma electrons. As a result, we have been able to obtain beam pulse compression data with minimal interference from the neutralizing plasma.

A second diagnostic, a Faraday cup, is used for measurements of the current. The Faraday cup is specially designed [23] to function in a plasma environment and to have good time resolution. It consists of hole plates with hole sizes comparable to the Debye length, in order to prevent plasma from entering into the cup. The cup geometry and external circuitry are optimized to assure fast time response ($\sim$3ns).

When the tilt voltage waveform is turned on, beam bunching is observed in the downstream diagnostic box. The degree of bunching, as well as the pulse shape, shown in Fig. 4, is clearly correlated with the voltage waveform, shown in Fig. 3. Theory specifies the ideal voltage waveform required to produce an exactly linear (versus z) velocity ramp [18, 19]. The tilt core waveform was optimized to obtain a rather close approximation to the ideal waveform as shown in Fig. 5. For a given voltage waveform, the position of maximal compression is changed as the beam energy is varied. A scan in beam energy demonstrates this behavior and is shown in Fig. 6.

Thus the maximum compression is observed by fine tuning the beam energy to match the voltage waveform and precisely position the longitudinal focal point at the diagnostic location. This is shown in Fig. 7. The $\sim$ 50 fold compression ratio, [see Fig. 7(b)], is obtained by taking the ratio of the signal with tilt voltage on (with compression) to the signal with tilt voltage off (without compression) [see Fig. 7(a)]. A similar result is measured with the Faraday cup as shown in Fig. 8. The LSP

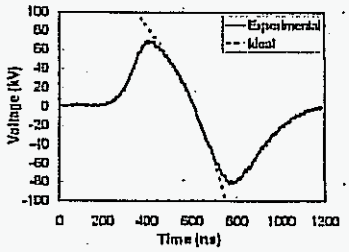

FIG. 5: Experimentally optimized and ideal induction module voltage waveforms.

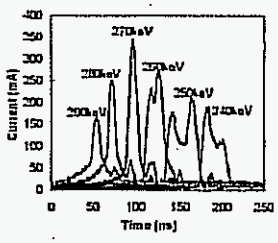

FIG. 6: Compressed beam current pulses using a nominal tilt core voltage waveform as the beam energy is varied.

simulation under these experimental conditions is shown in Fig. 9.

The strong effects of neutralization are evident by comparing the compression ratio with the plasma turned on and off. Figure 10 shows that the peak current is significantly reduced when the plasma is turned off. LSP simulations under similar conditions show qualitatively similar results.

Optical imaging has also been deployed to measure the transverse beam size as a function of time. We are able

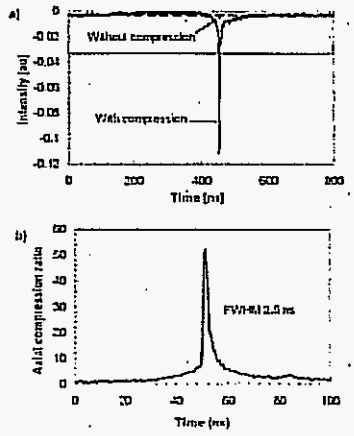

FIG. 7: (a) Measurements of beam signal using the phototube diagnostic for neutralized non-compressed, and neutralized compressed beams, and (b) compression ratio obtained from the measurements.

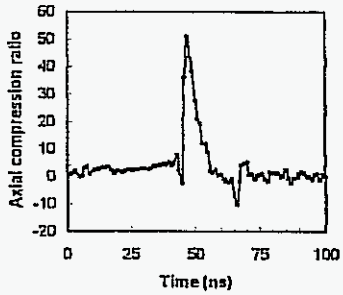

FIG. 8: Neutralized drift compression measurement using the Faraday cup.

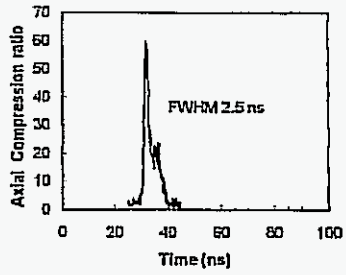

FIG. 9: LSP simulation of neutralized drift compression of a 25 mA K^+ beam using an ideal velocity tilt core waveform.

to measure the images with a 1 ns time resolution. It is interesting to observe that the transverse spot size is larger at the point of maximal compression, as shown in the Figs. 11(a) and 11(b). This feature is due to time-dependent defocusing effects occurring at the induction gap. The theory and simulations of this effect will be reported elsewhere.

Theory predicts that the nature of beam compression is strongly dependent on the drift length [18]. As the length is increased, the compression is more sensitive to the degree of neutralization. It is also more sensitive to the intrinsic longitudinal temperature of the ion beam.

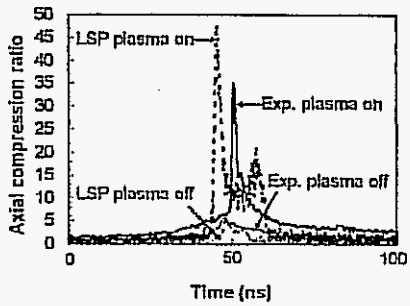

FIG. 10: Experimental data and LSP simulation of beam compression with neutralization (plasma source on) and without neutralization (plasma source off).

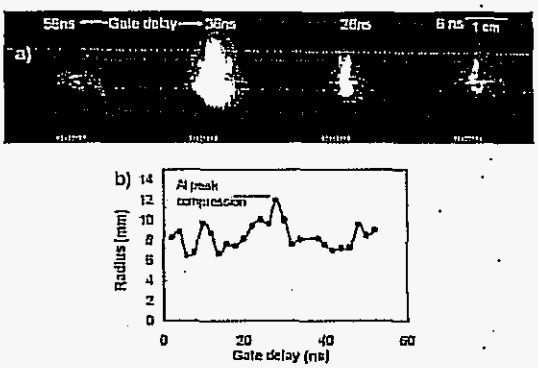

FIG. 11: Transverse images of neutralized compressed beam: (a) optical profile, and (b) beam radius. Note that the beam radius has increased at the point of maximum compression.

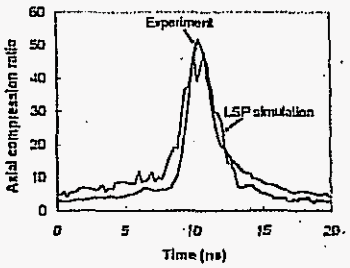

FIG. 12: Comparison of beam compression between experiment and LSP simulation for the 2-m long plasma column.

Finally, if there are any instabilities, e.g. two-stream, they may become evident with longer drift lengths. Although theory predicts two-stream effects to be benign, an experimental confirmation would be desirable.

For the above reasons, we have performed additional experiments with the drift length with plasma extended to two meters. We were able to recover the 50-fold compression in the 2-m experiment as shown in Fig. 12. The corresponding LSP simulation is also shown. If the compressed pulse length t_p were dominated by the longitudinal beam temperature T_l, t_p would be approximately given by

$$t_p = \frac{L}{v_l^2}\sqrt{\frac{2kT_l}{M}}, \qquad (1)$$

which yield roughly 3 ns for $T_l < 1eV$, where v_l, L, M and k are the mean longitudinal beam velocity, drift length, mass of ion and Boltzmann constant, respectively.

On the basis of this two-meter experiment we conclude that: 1) the degree of charge neutralization is sufficient to achieve 50 fold longitudinal compression while avoiding space-charge blow-up of the beam for the experimental configuration investigated; 2) the intrinsic longitudinal temperature is < 1eV; and 3) no collective instabilities have been observed.

Acknowledgments

This Research was supported by the U.S. Department of Energy under Contract No. DE-AC02-05CH11231 with the Lawrence Berkeley National Laboratory, and Contract No. DE-AC02-76CH03073 with Princeton Plasma Physics Laboratory. We thank Dr. A. Friedman, Dr. J. Barnard, Dr. C. Celata, Dr. I. Kaganovich, Dr. E. Lee, Dr. P. Seidl and Dr. W. M. Sharp for useful discussions and comments. Thanks also to Mr. D. Baca and Mr. D. L. Vanecek for useful technical assistance.

[1] S. S. Yu et al.,Nucl. Instrum. Meth. Phy. Res. A 544, 294 (2005).
[2] W. M. Sharp et al., Fusion Sci. Technol. 43, 393 (2003).
[3] D. R. Welch et al., Nucl. Instrum. Meth. Phys. Res. A 464, 134 (2001).
[4] W. M. Sharp et al., Nucl. Fusion 44, 221 (2004).
[5] S. S. Yu et al., in *Proc. of the 2003 Particle Accelerator Conf.*, edited by J.Chew, (IEEE, 2003), p. 98.
[6] E. Henestroza, et al., Phys. Rev. ST Accel. Beams 7, 083501 (2004).
[7] P. K. Roy et al., Phys. of Plasmas 11, 2890 (2004).
[8] B. G. Logan et al., Nucl. Fusion 45, 131 (2005).
[9] C. Thoma et al., Phys. of Plasmas 12, 043102 (2005).
[10] P. K. Roy et al., Nucl. Instrum. Meth. Phy. Res. A 544, 225 (2005).
[11] D. D.-M. Ho et al., Particle Accelerators 35, 15 (1991).
[12] T. Kikuchi et al., Phys. of Plasmas 9, 3476 (2002).
[13] M. J. L. de Hoon et al., Phys. of Plasmas 10, 855 (2003).
[14] H. Qin et al., Phys. Rev. ST Accel. Beams 7, 104201 (2004).
[15] R. C. Davidson and H. Qin, Phys. Rev. ST Accel. Beams 8, 064201 (2005).
[16] W. M. Sharp et al., Nucl. Instrum. Meth. Phys. Res. A 544, 398 (2005).
[17] W. M. Fawley et al., Phys. Plasmas 4, 880 (1997).
[18] D. R. Welch et al., Nucl. Instrum. Meth. Phys. Res. A 544, 236 (2005).
[19] C. Thoma et al., *Proc. of the 2005 Particle Accelerator Conf.*, in press (IEEE, 2005).
[20] A. Anders and G. Y. Yushkov, J. Appl. Phys. 91, 4824 (2002).
[21] A. Anders and R. A. MacGill, Surf. Coat. Technol. 133-134, 96 (2000).
[22] F. M . Bieniosek et al., Nucl. Instrum. Meth. Phy. Res. A 544, 268 (2005).
[23] A. Sefkow et al., *Proc. of the 2005 Particle Accelerator Conf.*, in press (IEEE, 2005).